Electron Photodetachment Dissociation of DNA Anions with Covalently or Noncovalently Bound Chromophores

Valérie Gabelica*, Frédéric Rosu, Edwin De Pauw

Mass Spectrometry Laboratory, Université de Liège, Institut de Chimie Bat. B6c, B-4000 Liège, Belgium.

Rodolphe Antoine, Thibault Tabarin, Michel Broyer, Philippe Dugourd

Université Lyon 1 ; CNRS ; LASIM, Bat. A. Kastler, 43 Bd du 11 Novembre 1918, F-69622 Villeurbanne, France.

* Email: v.gabelica@ulg.ac.be; Tel: +32-4-3663432; Fax: +32-4-3663413.

ABSTRACT

Double stranded DNA multiply charged anions coupled to chromophores were subjected to UV-Vis photo-activation in a quadrupole ion trap mass spectrometer. The chromophores included noncovalently bound minor groove binders (activated in the near UV), noncovalently bound intercalators (activated with visible light), and covalently linked fluorophores and quenchers (activated at their maximum absorption wavelength). We found that the activation of only chromophores having long fluorescence lifetimes did result in efficient electron photodetachment from the DNA complexes. In the case of ethidium-dsDNA complex excited at 500 nm, photodetachment is a multi-photon process. The MS^3 fragmentation of radicals produced by photodetachment at $\lambda = 260$ nm (DNA excitation) and by photodetachment at $\lambda > 300$ nm (chromophore excitation) was compared. The radicals keep no memory of the way they were produced. A weakly bound noncovalent ligand (m-amsacrine) allowed probing experimentally that a fraction of the electronic internal energy was converted into vibrational internal energy. This fragmentation channel was used to demonstrate that excitation of the quencher DABSYL resulted in internal conversion, unlike the fluorophore 6-FAM. Altogether, photodetachment of the DNA complexes upon chromophore excitation can be interpreted by the following mechanism: (1) ligands with sufficiently long excited state lifetime undergo resonant two-photon excitation to reach the level of the DNA excited states, then (2) the excited state must be coupled to the DNA excited states for photodetachment to occur. Our experiments also pave the way towards photodissociation probes of biomolecule conformation in the gas phase by Förster resonance energy transfer (FRET).

INTRODUCTION

A wide variety of activation methods can be used to fragment ions in tandem mass spectrometers [1]. Ion activation methods can be classified in the following way: collisions with neutrals (atoms, molecules or surfaces), collisions with ions (including proton and electron transfer reagents), collisions with electrons, and photo-activation. The most widely used method is collisional activation, because of its availability on all commercial tandem mass spectrometers. The DNA fragmentation pathways resulting from the various activation methods have been reviewed in 2004 [2]. Since then, some major advances must be mentioned in electron activation methods [3-5], and in infrared photodissociation [6].

We recently started exploring the gas-phase reaction pathways of multiply charged DNA single strands and double strands upon UV irradiation around 260 nm [7,8]. To our surprise, we found out that, instead of fragmentation, electron detachment was the major reaction pathway with strands containing guanines. Electron photodetachment itself is not useful for DNA structure analysis, but subsequent collisional activation of the oligonucleotide radicals produced by electron photodetachment gives fragmentation into w, d, a• and z• ions with good sequence coverage [7]. This technique combining electron photodetachment and collision-induced dissociation was coined EPD (electron photodetachment dissociation). It has now been shown to apply to peptides and proteins as well [9].

Apart from the sequencing applications of EPD, numerous questions remain about the electron photodetachment mechanism, and how it compares with electron detachment dissociation [3-5] and thermal electron detachment [10,11]. We will briefly summarize our current understanding of the photodetachment mechanism [8]. The electron binding energy in multiply charged DNA anions depends on the balance between electron binding energy of the different DNA constituents (the phosphates, the sugars, and the bases) and the Coulombic repulsion between like charges [10-12]. It has been shown that in a negatively charged environment, the electron binding energy of the nucleic bases can become lower than the electron binding energy of the phosphate groups, and that the highest

occupied molecular orbital (HOMO) can be located on the bases [13-15]. Guanine is the base with the lowest ionization energy, followed by adenine, cytosine, and finally thymine. If the photon energy (for λ = 260 nm, hν = 4.77 eV) is superior to energy difference between the even-electron parent ion and the anion radical with one electron fewer (this energy difference is defined as the electron binding energy, or BE), electron photodetachment can occur. If the photon energy is superior to the electron binding energy plus the repulsive Coulomb barrier (BE+RCB), photodetachment can be very fast. If the photon energy falls between BE and BE+RCB, electron photodetachment can still proceed via tunneling through the barrier. The other key point in the mechanism is that electron photodetachment proceeds via some specific electronic excited states corresponding to base excitation. This is suggested by the wavelength-dependence, which shows maximum photodetachment efficiency around 260 nm and a drop-off at higher photon energies (shorter wavelengths).

In the present paper, we report further photo-activation experiments on DNA complexes with chromophores absorbing at different wavelengths than the nucleic bases. We investigated the noncovalently bound and the covalently bound chromophores shown on Scheme 1. Two kinds of noncovalent ligands were tested: minor groove binders (these ligands interact with DNA mainly by hydrogen bonding with the sides of the base pairs), and intercalators (these ligands stack between base pairs and interact mainly via electrostatic dipole-dipole interactions). We also investigated one covalently linked fluorophore (6-FAM, an analog of fluorescein which is more photostable) and one covalently linked quencher (DABSYL). In a fluorophore, following photon absorption, the initial excited state relaxes into a lower lying excited state from which light is re-emitted. In a photostable quencher, all electronic energy is converted into vibrational energy. In the case of azobenzenes like DABSYL, the relaxation to the electronic ground state involves trans-cis isomerization of the N=N bond [16]. Azobenzene chromophores can therefore be used to locally deposit vibrational internal energy and probe its redistribution over the biomolecule [17]. The general aim was to discover whether chromophore-specific photochemical reactions might be observed. The underlying questions relate to

the efficiency of internal energy redistribution from specific electronically excited to vibrationally excited states, and to the efficiency of intramolecular energy redistribution in large biomolecules including non-covalently bound partners, when the energy is initially located in one well-defined chromophore [18-24]. We show here that for some of the chromophores, photodetachment is the major photochemical pathway, like for the nucleic bases [7,8]. We also found some evidence of internal energy redistribution over the whole biomolecule ions. The relationship between de-excitation channels, the lifetime of excited states of the chromophores, and electron photodetachment of the DNA-chromophore complexes is also discussed.

MATERIALS AND METHODS

Materials

All DNA single strands were purchased from Eurogentec (Angleur, Belgium) and used without further purification. The duplex $d(CGCGAATTCGCG)_2$ (noted dsB like in some of our previous papers) was prepared by mixing 100 µM single strand in 100 mM aqueous NH_4OAc to yield a 50 µM duplex stock solution. The hairpin-forming oligonucleotide sequence dCCAGGTCTGAGGCGTCCTGG was purchased from Eurogentec in three different forms: unmodified, modified with DABSYL on the 3' end, or modified with 6-FAM on the 5' end. Hairpin formation was ensured by storing the oligonucleotide in 100 mM NH_4OAc. All ligands were purchased from Sigma–Aldrich (www.sigma-aldrich.com). The drug stock solutions were prepared in bi-distilled water, except m-Amsacrine which was dissolved in methanol. DNA-ligand mixtures were prepared at 10-10 µM or 10-20 µM in 100 mM NH_4OAc, with 20% methanol added just before spraying.

Mass Spectrometry

All experiments were performed on an commercial LCQ Duo quadrupole ion trap mass spectrometer (ThermoFinnigan, San Jose, CA), coupled to a Panther^{TM} OPO laser pumped by a 355-nm Nd:YAG PowerLite^{TM} 8000 (5 ns pulse width, 20 Hz repetition rate). The vacuum chamber and the central ring electrode of the mass spectrometer were modified to allow the injection of UV and visible lights [25]. An optical fiber glued to the ion trap opposite to the incoming beam was used for laser alignment, ensuring reproducible overlap between the laser beam and the ion cloud. In the visible region (410-700 nm), the signal wave of the OPO was used. Frequency doubling of the signal wave allows reaching the UV range 215-320 nm. There is a gap between 320 nm and 410 nm, where the only possibility was to use the 355-nm Nd:YAG laser (after attenuation). A cylindrical lens (f = 500 mm), located ~500 mm from the center of the trap, is used to reduce the ellipticity of the laser beam. The standard electrospray source was operated as described previously [7,8]. To perform laser irradiation for a given number of laser pulses, we add an MS^n step with activation amplitude of 0%, during which a shutter located on the laser beam is open. This electromechanical shutter triggered on the RF signal of the ion trap synchronizes the laser irradiation with the MS/MS events conducted in the ion trap.

RESULTS

Noncovalently bound chromophores

We have shown previously that DNA single strands and double strands undergo electron photodetachment when using laser wavelengths matching nucleic acid base absorption (maximum between 250 and 270 nm). In the present study we explored the relaxation pathways following photo-activation of DNA-ligand noncovalent complexes using wavelengths corresponding to ligand electronic excitation. The ligands tested here are listed in Table 1, together with their known absorption and

fluorescence properties in solution. The initial choice of working wavelengths was done by assuming that ligand absorption in the gas phase DNA complexes occurs at similar wavelengths than ligand absorption in the solution phase DNA complexes. Then, when laser tuning was possible, we checked that the same pathways are also observed at wavelengths above and below the initially chosen wavelength, to check for possible shifts in the absorption maxima.

We studied here four minor groove binding ligands: netropsin, Hoechst 33258, DAPI and berenil. When bound to DNA, all have their maximum absorption wavelength in the range 320-370 nm, where DNA alone does not absorb. For netropsin, we performed laser excitation experiments at 310 nm, and for the other three dyes we used the 355-nm laser. The results are shown in Figure 1(a-d), and in supporting information (SI). With netropsin, very little electron photodetachment is observed at 310 nm even after irradiation during 5 seconds (100 laser pulses) at 6.5 mW (see SI). Control experiments show that when irradiating the duplex DNA alone in the same conditions, no photodetachment is observed.

At 355 nm, the Nd:YAG laser was attenuated to 30 mW to perform the laser excitation experiments. Figure 1(a) shows that even for the duplex DNA alone, some electron photodetachment occurs. This spectrum constitutes the background spectrum for Figures 1(b-d). We can see in Figure 1(b) that when one molecule of Hoechst 33258 is noncovalently bound to the duplex DNA, photodetachment at 355 nm is dramatically enhanced. The photodetachment yield is lesser with the ligand DAPI, but it is nevertheless significant (Figure 1c). When two molecules of DAPI are bound to the duplex DNA instead of one, the photodetachment yield seems more than doubled (Figure 1d). It must be mentioned at this stage that, although the first binding site is most probably minor groove binding in the vicinity of the AATT site, the binding mode of the second molecule is probably intercalation [40,41], because the doubly charged DAPI in the minor groove is likely to prevent binding of a second molecule in its vicinity.

At this stage we have two ligands (Hoechst 33258 and DAPI) provoking significant electron photodetachment, and one ligand (netropsin) provoking almost no electron photodetachment. As

Hoechst 33258 and DAPI are fluorescent when bound to DNA while netropsin is not, we hypothesized that the photodetachment mechanism could be related to ligand fluorescence. However, the comparison between netropsin and the other ligands is difficult because of the limited laser power at 310 nm (at 355 nm the netropsin complex gave no photodetachment either, see SI). We therefore used berenil, a nonfluorescent minor groove binder that absorbs significantly at 355 nm when bound to DNA (absorption maximum is at 370 nm). Even after 3s irradiation, no photodetachment is observed (see SI).

We also investigated the photoactivation spectra of three intercalating molecules. Intercalators are usually polyaromatic compounds which absorb at $\lambda > 400$ nm. Experiments with doxorubicin and m-amsacrine at various wavelengths around their reported absorption maximum did not show significant electron photodetachment (see SI). The ligand ethidium, however, showed significant electron photodetachment efficiencies from 490 to 550 nm. Photodetachment spectra recorded at 550 nm for the complexes with one and two ethidium molecules are shown in Figures 1(e) and 1(f), respectively. When two ethidium molecules are present in the complex, the photodetachment yield is doubled. The binding sites are supposed to be equivalent (intercalation of both ligands in the 2:1 complex). Ethidium is fluorescent when bound to DNA. Free doxorubicin is fluorescent, but on the contrary to ethidium, Hoechst 33258 and DAPI, fluorescence quenching occurs upon DNA binding [33,35]. m-Amsacrine is not fluorescent.

m-Amsacrine as a probe of internal energy uptake upon laser irradiation

While exploring the pathways of the m-amsacrine ligand, we made an interesting observation. m-amsacrine is a very loosely bound noncovalent ligand which is lost as a neutral at low collision energies when MS/MS is performed on the DNA complexes [42], and we propose to use it as a messenger to probe the vibrational internal energy uptake. This kind of strategy involving the loss of a weakly bound neutral [43] or ion [44] has been used by others for infrared spectroscopy. No significant

photodetachment or photodissociation is observed when using wavelengths between 400 and 500 nm. However, when irradiating the $[dsB+amsacrine]^{5-}$ complex with 260-nm light, loss of neutral ligand was observed. Figure 2(a) shows the photodetachment spectrum of the complex $[dsB+amsacrine]^{5-}$, irradiated at 260 nm during 600 ms. In addition to electron photodetachment, loss of ligand is observed from the closed shell 5- ion (i.e. from the parent ion) and from the resulting •4- radical. We checked that when the $[dsB+amsacrine]^{5-}$ complex is left for 600 ms in the ion trap without laser activation, no spontaneous ligand loss occurs. Loss of neutral amsacrine therefore indicates some internal energy uptake by the closed shell species that did not undergo photodetachment, and also by the radical species produced by photodetachment. This confirms that internal conversion must indeed be taken into account in the energy relaxation mechanisms following DNA excitation at 260 nm [8].

m-Amsacrine can therefore be used as a probe of internal energy uptake upon irradiation of other chromophores as well. Due to the limited mass range (*m/z* max. 2000), this experiment could be performed only with the ethidium complex. The duplex dsB was mixed in solution with the two ligands ethidium (E) and m-amsacrine (A). The mixed complex $[dsB+E+A]^{5-}$ at m/z = 1597.4 was isolated and subjected to laser irradiation at 550 nm, corresponding to ethidium absorption. As can be seen on Figure 2(b), loss of the m-amsacrine ligand occurs only to a small extent.

Covalently linked chromophores

We tested a commercially available fluorophore (6-FAM) and a commercially available quencher (DABSYL), linked to a hairpin-forming DNA 20-mer. The results for the fluorophore FAM at 490 nm and the quencher DABSYL at 450 nm are shown in Figure 3. Both the fluorophore-labeled and the quencher-labeled DNA show a very tiny amount of •4- radical indicating some photodetachment from the 5- closed shell parent ion (Figures 3(a) and 3(b), respectively). Control spectra using the unlabeled hairpin under the same laser irradiation conditions (see SI) show no photodetachment at all, confirming

that photodetachment was due to the covalently linked chromophore. To ensure that no significant photodetachment was observable, experiments were also performed on the 6- charge state, which should be even more sensitive to electron detachment than the 5- charge state because of coulombic repulsion. The laser wavelength was tuned from 440 nm to 560 nm, but no photodetachment is detected (see SI).

It can be noted that the spectrum obtained with the quencher (Figure 3b) is noisier than all other photodetachment spectra, indicating possible fragmentation of the DNA strand. But an obvious problem is the large number of vibrational degrees of freedom (> 2000) in the system, among which the 2.76 eV of each 450-nm photon absorbed by the quencher can be redistributed. Even if energy redistribution among all vibrational degrees of freedom is not complete before fragmentation, many fragmentation channels can possibly be accessed, resulting in a noisy spectrum and inefficient detection of quencher absorption. With the aim of creating one low-energy dissociation channel that would be easier to detect than DNA fragmentation, we added the noncovalent intercalator m-amsacrine to the hairpin. There are five base pairs in the hairpin stem, and therefore four potential intercalation sites.

The spectra of the unlabeled hairpin complexed with m-amsacrine at 490 nm and 450 nm show no ligand-induced photodetachment at 490 nm, and a very small ligand-induced photodetachment at 450 nm (see SI). Upon irradiation of the FAM-hairpin complex with m-amsacrine (Figure 3c), the amount of photodetachment is the same as for the FAM-hairpin alone. More importantly, no loss of neutral ligand is observed, indicating that there was no significant internal energy uptake by the FAM-hairpin. However, upon irradiation of the DABSYL-hairpin complex with m-amsacrine (Figure 3d), loss of neutral ligand from the parent ion is clearly observed, indicating internal energy uptake by the DABSYL-hairpin upon laser irradiation. Overall, our results suggest that, as expected from the solution-phase behavior, the fluorophore absorbs and re-emits light, while the quencher absorbs light and converts it into vibrational energy.

MS³ of radical ions as a function of the wavelength used for photodetachment

Finally, in order to determine whether the radical produced by electron photodetachment keeps some memory of the chromophore that was excited, we compared the CID spectra of the $[dsB+Ligand]^{\bullet 4-}$ radicals resulting of electron photodetachment from the $[dsB+Ligand]^{5-}$ complexes. The CID spectra of the $[dsB+Ligand]^{\bullet 4-}$ radicals were also compared to the CID spectra of the $[dsB+Ligand]^{4-}$ closed shell species. Figure 4 shows these MS³ spectra in the *m*/*z* range 1800-1950. No fragment ion was observed outside this range. Figure 4(a) shows the CID spectrum of the $[dsB+Hoechst\ 33258]^{4-}$ closed shell species. Figure 4(b) shows the CID spectrum of the $[dsB+Hoechst\ 33258]^{\bullet 4-}$ radical coming from photodetachment at 260 nm (excitation of the DNA chromophore), and Figure 4(c) shows the CID spectrum of the $[dsB+Hoechst\ 33258]^{\bullet 4-}$ radical coming from photodetachment at 355 nm (excitation of the ligand chromophore). As expected, CID of the radicals results in different fragments than CID of the closed shell species. In addition to the losses of H_2O, CO, neutral base, neutral $z_1\bullet$ and $a_1\bullet$ fragments already reported for dsDNA alone [7], we observe neutral losses of ≈ 44 Da and ≈ 58 Da. These correspond to small neutral losses from the ligand, e.g. loss of $CH_3N^{\bullet}CH_3$, and of $CH_3N^{\bullet}CH_2CH_3$. However, the similarity between spectra 4(b) and 4(c) clearly indicates that the radicals keep no memory of which chromophore was excited. A similar conclusion is reached in the case of ethidium: fragmentation of the radical produced by DNA excitation at 260 nm (Figure 4(e)) is the same as the fragmentation of the radical produced by ethidium excitation at 550 nm (Figure 4(f)). The major difference with fragmentation of the closed shell 4- species (Figure 4(d)) is the observation of neutral ethidium loss when the 4- radical is subjected to CID. In closed shell species, ethidium always remains positively charged and never exits the complex as a neutral. The mass resolution and accuracy does unfortunately not allow determining the oxidation state of the resulting fragment $[dsB]^{4-}$. Future investigation of oxydation/reduction reactions of the ligand and DNA upon photoactivation would help refine the relaxation mechanisms.

DISCUSSION

Mechanism of electron photodetachment following chromophore irradiation

The mechanism must take the following observations into account. First, among chromophores noncovalently bound to the DNA, only those with a significantly long fluorescence lifetime (> 1 ns) are able to provoke electron photodetachment from the complex. However, when the fluorophore 6-FAM is covalently attached to the DNA extremities by an alkyl linker, it is unable to provoke electron photodetachment. Danell et al. [45] performed fluorescence counting experiments on BODIPY® TMR-X and BODIPY® TR-X upon 532-nm laser irradiation. Electron photodetachment was detected, and the authors subsequently found that this was due to a thermal autodetachment following internal energy input by the laser excitation. Thermal electron detachment was also observed in the absence of laser and chromophores, just by heating the ions in the trap.

The first question is the single-photon or multi-photon character of electron photodetachment with chromophores. In the case of ethidium, excitation with 550-nm light corresponds to 2.25 eV/photon, and in the case of the minor groove binders, 355-nm light corresponds to 3.49 eV/photon. We examined the power dependence of photodetachment yield for ethidium at 500 nm (2.48 eV), where electron photodetachment is a little more efficient, to allow single laser pulse experiments. The results in Figure 5 clearly show that photodetachment is a multiphoton process. First, there is an energy threshold below which no photodetachment is observed. A single-photon process would have resulted in a linear dependence of the photodetachment yield on the laser energy, with an intercept at (0,0). Second, the series obtained with different number of laser pulses do not overlap, indicating that for a given total fluence, higher photodetachment efficiency is achieved if this energy is given in one pulse than several pulses. This suggests that, on the contrary to 260-nm photodetachment which is a single-photon process

[8] (mechanism represented in Figure 6(a)), electron photodetachment following ligand excitation at 550 nm is a multi-photon process.

Therefore, the fact that only ligands having long fluorescence lifetimes can provoke electron photodetachment can be understood as follows. The ligand must remain long enough in an excited state in order to have a significant probability to absorb a second photon during the laser pulse, which lasts for 5-7 ns. Chromophores with too short excited state lifetime will convert back to the ground state before absorption of the second photon can occur, as depicted in Figure 6(b). The quenching occurs via internal conversion of electronic energy into vibrational energy and the parent ion accumulates vibrational energy, as demonstrated in the case of the quencher DABSYL via m-amsacrine loss.

Chromophores with excited states having nanosecond lifetimes, however, can absorb a second photon from their excited state within the nanosecond laser pulse (Resonant Two-Photon Excitation). In the case of ethidium, the chromophore with the longest photodetachment wavelengths measured to date, two 550-nm photons make 4.50 eV (equivalent to one 275-nm photon), which is sufficient to reach the DNA excited states [8]. The experiment with the ethidium complex bearing the m-amsacrine reporter (Figure 2(b)) showed that internal energy remaining in the radical ion after photodetachment at 550 nm is low.

The next question is why the fluorophore 6-FAM coupled to the DNA via an alkyl linker does not provoke electron photodetachment? This observation suggests that a second requisite for photodetachment to occur is a coupling between the chromophore excited states and the DNA excited states. An alkyl spacer between the fluorophore and the DNA would prevent such coupling. Fluorescein is known to be very mobile when attached to DNA or RNA [46], and is probably not stacked on the terminal bases. In contrast, the excited states of noncovalently bound ligand fluorophores appear to be coupled more effectively to the DNA excited states, so that electron photodetachment from the 5-complex can proceed. In our MS^3 experiments, radicals seem to keep no memory of which chromophore was excited (Figure 4). Although it is tempting to conclude that this result supports the

hypothesis that similar excited states are involved in 260-nm photodetachment and ligand-mediated photodetachment, experiments with much shorter delays between photodetachment and fragmentations would be needed, because radical rearrangements can occur between the MS^2 and the MS^3 steps. The mechanism for the covalently bound fluorophore (noted F) is represented in Figure 6(c), and that for the noncovalently bound fluorophores (noted L) is represented in Figure 6(d). Further experiments with intercalating chromophores covalently linked to the DNA strands would help understanding the differences.

The exact nature of the coupling between the ligand excited states and the DNA excited states remains an open question. It must nonetheless be noted that electron transfer from the excited ligand to the DNA is unlikely: the ligands are positively charged, and ligands like ethidium are actually known to be better electron acceptors in their excited state than in their ground state [47]. The hypothesis of electron transfer from the DNA to the excited chromophore might be considered given the huge amount of literature about charge transfer in DNA where hole injection is controlled by chromophores stacked between the DNA bases [48]. Ethidium is precisely one of the chromophores that can be used for provoking charge transfer in DNA [49,50], but doxorubicin is an even more efficient DNA oxidant than ethidium [48], which is not in line with our experiments. Furthermore, chromophores must be stacked above or between DNA base pairs for long-distance charge transfer to occur. In other terms, this can only happen with intercalating molecules and not with minor groove binders. In control experiments with ethidium and DAPI complexes with single-stranded 12-mer DNA, photodetachment upon chromophore excitation was also observed (data not shown). Therefore, our electron photodetachment experiments are against long range DNA-to-chromophore electron transfer as the initiator of electron photodetachment and we propose in Figure 6(d) that the detachment involves an energy transfer from the electronic excited state of the Ligand to DNA excited states. This electronic coupling is most probably sensitive not only to the ligand excited state lifetime, but also to the nature of the binding site. For example, for Hoechst 33258 and DAPI complexes, although excited state lifetimes are similar, the

photodetachment yields differ significantly. Further experiments and calculation are needed to decipher the nature of the coupling between ligand and DNA excited states. A particularly interesting question is whether the photodetachment spectra (photodetachment yields as a function of the wavelength) can be related to the biomolecule conformation and to the ligand binding mode or binding site.

Electronic-to-vibrational energy conversion: towards photodissociation probes of gas-phase ion structure?

In instances where fast photodetachment does not take place, internal conversion of the electronic internal energy into vibrational internal energy can occur. The energy is initially localized in the excited chromophore, and then redistributes over all degrees of freedom. Fragmentation channels occurring before complete intramolecular vibrational energy redistribution (IVR) over the entire species (non-ergodic case) should be indicative of the proximal environment of the chromophore. An example of conformation-specific photodissociation probes has been demonstrated in peptides labeled with benzophenone, which showed CO_2 loss when the C-terminus was in contact with to the chromophore [51]. Unfortunately, with the ligands studied here, no particular photodissociation channels could be observed, and complete IVR seems to take place. The only way to detect the increase in vibrational internal energy once it is redistributed over all degrees of freedom is to use a loosely bound reporter [43,44], such as m-amsacrine in the present case.

Of course once the energy is delocalized over the entire molecule, the fragmentation itself is not indicative of the local environment. Then, a donor-acceptor configuration can be used instead, based on Förster resonance energy transfer (FRET, also often named "fluorescence resonance energy transfer"). FRET is a nonradiative energy transfer from one molecule (a fluorescent donor) to another (the acceptor) [52]. Although it is a nonradiative process, its efficiency is maximum when the emission wavelength of the donor matches the absorption wavelength of the acceptor. As FRET efficiency

depends on the donor-acceptor distance (in $1/r^6$), FRET is commonly used to probe the conformation of biomolecules in solution, including nucleic acids [53]. Several groups developed specialized instrumentation to allow fluorescence measurements in trap mass spectrometers [54-56], and probing gas phase ion conformation either by measuring changes in the donor fluorescence [45,57], or by measuring the acceptor fluorescence [58]. Here we propose using a fluorophore as the donor and a quencher as the acceptor, in a configuration known as a "molecular beacon" [59,60]. In solution, energy absorption by the quencher diminishes the fluorescence of the donor. In the case of ions isolated in the gas phase, energy absorption by the quencher would result in electronic-to-vibrational energy conversion and ion fragmentation. Then, using a loosely bound neutral as reporter, internal energy conversion with quenchers can be detected even in large biomolecules. Our experiment with the weakly bound intercalator m-amsacrine and the quencher DABSYL show that it might be possible to probe biomolecule conformation by combining FRET and photodissociation. Detecting the onset of a fragmentation signal can be much more sensitive than direct fluorescence counting in the mass spectrometer, but most of all it can be more readily implemented in commercial mass spectrometers, as photodissociation probes only require the coupling of a light source to the mass analyzer.

ACKNOWLEDGMENTS

The GDR 2758 CNRS "Agrégation, fragmentation et thermodynamique des systèmes complexes isolés". is acknowledged for financial support. V. G. is an FNRS research associate and F. R. is an FNRS postdoctoral fellow (Fonds National de la Recherche Scientifique, Belgium).

Table 1. Absorption and fluorescence properties of the chromophores: λ_{max} = wavelength of maximum absorption; λ_{em} = wavelength of maximum fluorescence emission; λ_{ex} = excitation wavelength; Φ = fluorescence quantum yield; τ = fluorescence lifetime. Properties in water unless mentioned otherwise.

Chromophore	**Chromophore alone**		**Chromophore bound to dsDNA**		
	λ_{max}	**Fluorescence**	**Binding mode**	**λ_{max}**	**Fluorescence**
Hoechst 33258	337 nm [26,27]	λ_{em} = 508 nm, Φ = 0.015 τ = 0.20 ns [26] λ_{em} = 475 nm Φ = 0.02 (λ_{ex} = 340 nm) [27]	Minor groove	349 nm [26] 360 nm [27] 355 nm [28]	λ_{em} = 458 nm Φ = 0.42 τ = 1.94 ns [26] λ_{em} = 485 nm Φ = 0.3 (λ_{ex} = 340 nm) [27]
DAPI	341 nm [26]	λ_{em} = 496 nm Φ = 0.019 τ = 0.16 ns [26]	Minor groove	356 nm [26]	λ_{em} = 455 nm Φ = 0.34 τ = 2.20 ns [26]
Netropsin	296 nm [29]	Not fluorescent	Minor groove	320 nm [30]	Not fluorescent
Berenil	370 nm [31]	Not fluorescent	Minor groove		Not fluorescent
Ethidium	479 nm [26]	λ_{em} = 632 nm Φ = 0.039 τ = 1.56 ns [26]	Intercalation	520 nm [26,32]	λ_{em} = 608 nm Φ = 0.35 τ = 28.3 ns [26]
Doxorubicin (quinizarin chromophore is the same as for daunomycin)	2 maxima: 473 and 494 nm [33]	λ_{em} = 552 nm [34] λ_{em} = 590 nm (λ_{ex} = 400 nm) [33] τ_1 = 0.63 ns (23%) τ_2 = 1.1 ns (77%) [33]	Intercalation	Daunomycin: 505 nm [35]	Daunomycin: λ_{em} = 555 nm (λ_{ex} = 480 nm) [35] Fluorescence quenching (fluorescence relative to free chromophore = 0.05) [35]
m-Amsacrine	434 nm (MeOH)	Not fluorescent	Intercalation		Not fluorescent
DABSYL	453 nm (MeOH) [36]	Not fluorescent	Covalenty linked (3' end)	475 nm [37]	Not fluorescent
6-FAM (data from fluorescein)	490.5 nm [38]	λ_{em} = 515 nm [38], Φ = 0.92 [38,39] τ = 4.16 ns [39]	Covalently linked (5' end)	494 nm [37]	Supposedly similar as free chromophore

FIGURE LEGENDS

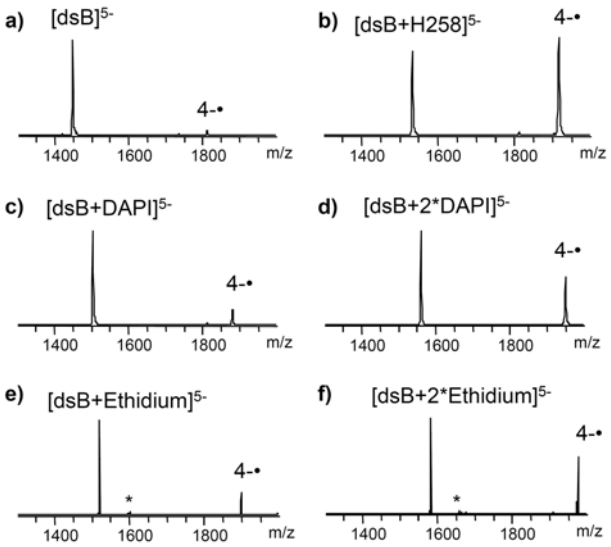

Figure 1. MS/MS spectra on the duplex dsB (sequence: $[dCGCGAATTCGCG]_2$) complexes with ligands at different wavelengths for the charge state 5-. (a-d): MS/MS during 1 s at 355 nm (30 mW at OPO exit) on dsB alone (a), dsB + Hoechst 33258 (b), dsB + DAPI (c), dsB + 2×DAPI (d). (e-f): MS/MS during 2 s at 550 nm (90 mW at OPO exit) on dsB + ethidium (e), dsB + 2×ethidium (f). Asterisks indicate neutral adducts on the parent ion occurring upon long ion storage.

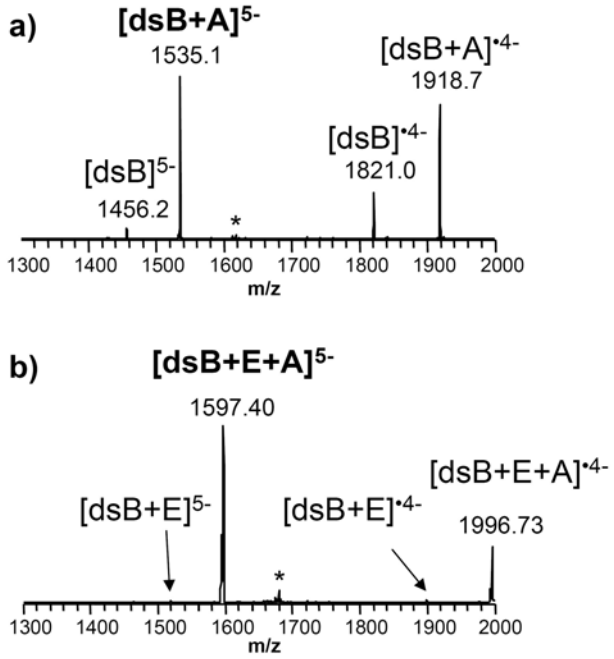

Figure 2. (a) MS/MS during 600 ms at 260 nm (16 mW at OPO exit) on [dsB + m-amsacrine]$^{5-}$ at *m*/*z* = 1535.1. (b) MS/MS during 5 s at 550 nm (70 mW at OPO exit) on [dsB + Ethidum + m-amsacrine]$^{5-}$ at *m*/*z* = 1597.4. dsB = d(CGCGAATTCGCG)$_2$; A = m-amsacrine; E = ethidium. Asterisks indicate neutral adducts on the parent ion occurring upon long ion storage.

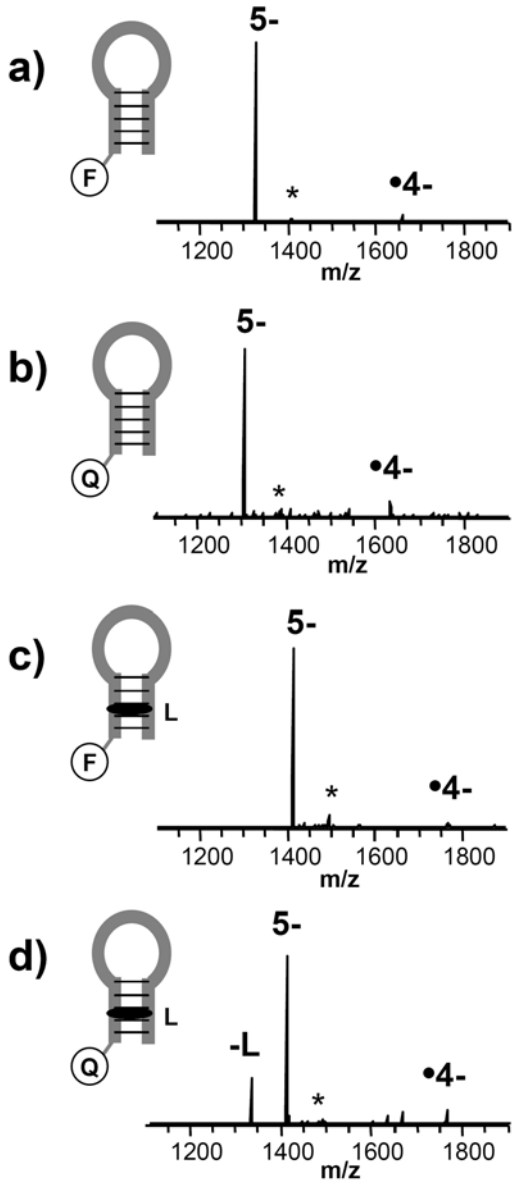

Figure 3. MS/MS spectra obtained by 4 second laser irradiation of a DNA hairpin with covalently linked fluorophore 6-FAM (noted F) and quencher DABSYL (noted Q), with and without ligand m-amsacrine (noted L). (a) FAM-hairpin conjugate irradiated at 490 nm. (b) DABSYL-hairpin conjugate irradiated at 450 nm . (c) FAM-hairpin conjugate complex with m-amsacrine irradiated at 490 nm. (d) DABSYL-hairpin conjugate complex with m-amsacrine irradiated at 450 nm Asterisks indicate neutral adducts on the parent ion occurring upon long ion storage.

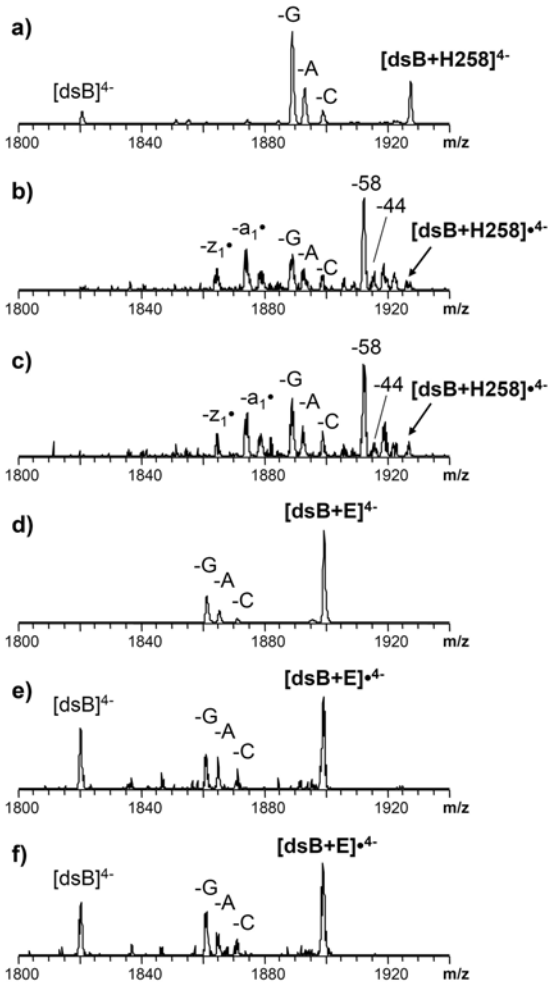

Figure 4. Comparison of CID of closed shell and radical ions from the ligand-DNA complexes. (a) CID during 30 ms at 10% activation amplitude on [dsB+Hoechst 33258]$^{4-}$ produced by electrospray. (b) CID during 30 ms at 10% activation amplitude on [dsB+Hoechst 33258]$^{\bullet 4-}$ produced by electron photodetachment of [dsB+Hoechst 33258]$^{5-}$ under 2-s irradiation at 260 nm. (c) CID during 30 ms at 10% activation amplitude on [dsB+Hoechst 33258]$^{\bullet 4-}$ produced by electron photodetachment of [dsB+Hoechst 33258]$^{5-}$ under 5-s irradiation at 355 nm. (d) CID during 30 ms at 9% activation amplitude on [dsB+Ethidium]$^{4-}$ produced by electrospray. (e) CID during 30 ms at 9% activation amplitude on [dsB+Ethidium]$^{\bullet 4-}$ produced by electron photodetachment of [dsB+Ethidium]$^{5-}$ under 2-s irradiation at 260 nm. (f) CID during 30 ms at 9% activation amplitude on [dsB+Ethidium]$^{\bullet 4-}$ produced by electron photodetachment of [dsB+Ethdium]$^{5-}$ under 2-s irradiation at 550 nm.

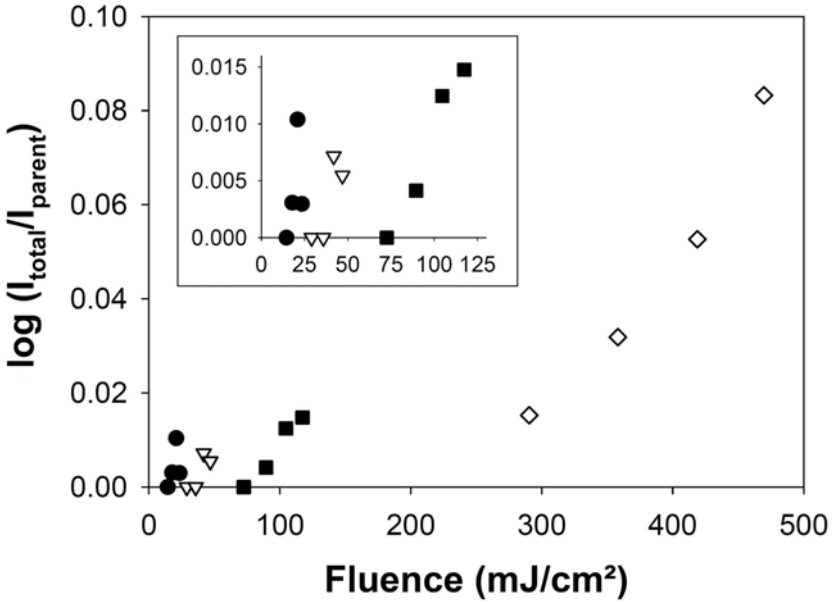

Figure 5. Relative photodetachment yield of [dsB+Ethidium]$^{5-}$ at 500 nm as a function of the total laser fluence (fluence per laser pulse multiplied by the number of pulses). Black circles = 1 laser pulse, white triangles = 2 laser pulses, black squares = 5 laser pulses and white diamonds = 20 laser pulses. The inset shows a zoom on the low fluence region.

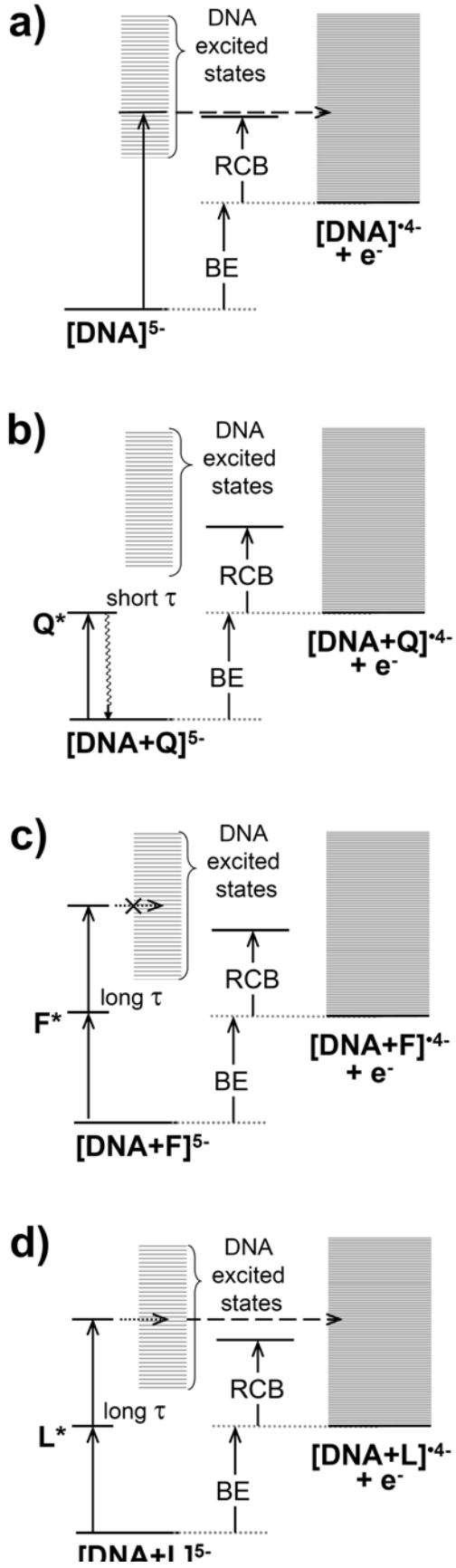
a)
DNA
excited
states
RCB
[DNA]•4-
+ e-
BE
[DNA]5-
b)
DNA
excited
states
RCB
short τ
Q*
[DNA+Q]•4-
+ e-
BE
[DNA+Q]5-
c)
DNA
excited
states
RCB
long τ
F*
[DNA+F]•4-
+ e-
BE
[DNA+F]5-
d)
DNA
excited
states
RCB
long τ
L*
[DNA+L]•4-
+ e-
BE
[DNA+L]5-

Figure 6. Photodetachment mechanism proposed in the DNA complexes. (a) DNA excited around 260 nm results in electron photodetachment. (b) DNA complex with a quencher Q excited at the quencher absorption wavelength results in internal conversion back to the ground state. (c) DNA linked with a fluorophore F can absorb two photons, but if coupling to the DNA excited states is not efficient, no photodetachment occurs. (d) DNA with noncovalently bound fluorophore ligands L can absorb two photons and electron photodetachment occurs via coupling with the DNA excited states. BE = electron binding energy; RCB = repulsive Coulomb barrier. (In these schemes, the values of BE and RCB, in particular the position of RCB as compared to excited states, are not known. They depend on the observed complexes, their exact conformation, and the photon energy)

References

1. Sleno, L.; Volmer D. A. Ion activation methods for tandem mass spectrometry. *J. Mass Spectrom.* **2004**, *39*, 1091-1112.

2. Wu, J.; McLuckey S. A. Gas-phase fragmentation of oligonucleotide ions. *Int. J. Mass Spectrom.* **2004**, *237*, 197-241.

3. Mo, J. J.; Hakansson K. Characterization of nucleic acid higher order structure by high-resolution tandem mass spectrometry. *Anal. Bioanal. Chem.* **2006**, *386*, 675-681.

4. Yang, J.; Hakansson K. Fragmentation of oligoribonucleotides from gas-phase ion-electron reactions. *J. Am. Soc. Mass Spectrom.* **2006**, *17*, 1369-1375.

5. Yang, J.; Mo J. J.; Adamson J. T.; Hakansson K. Characterization of oligodeoxynucleotides by electron detachment dissociation Fourier transform ion cyclotron resonance mass spectrometry. *Anal. Chem.* **2005**, *77*, 1876-1882.

6. Wilson, J. J.; Brodbelt J. S. Infrared multiphoton dissociation of duplex DNA/drug complexes in a quadrupole ion trap. *Anal. Chem.* **2007**, *79*, 2067-2077.

7. Gabelica, V.; Tabarin T.; Antoine R.; Rosu F.; Compagnon I.; Broyer M.; De Pauw E.; Dugourd P. Electron Photodetachment Dissociation of DNA Polyanions in a Quadrupole Ion Trap Mass Spectrometer. *Anal. Chem.* **2006**, *78*, 6564-6572.

8. Gabelica, V.; Rosu F.; Tabarin T.; Kinet C.; Antoine R.; Broyer M.; De Pauw E.; Dugourd P. Base-Dependent Electron Photodetachment from Negatively Charged DNA Strands upon 260-nm Laser Irradiation. *J. Am. Chem. Soc.* **2007**, *129*, 4706-4713.

9. Antoine, R.; Joly L.; Tabarin T.; Broyer M.; Dugourd P.; Lemoine J. Photo-induced formation of radical anion peptides. Electron photo-detachment dissociation experiments. *Rapid Commun. Mass Spectrom.* **2007**, *21*, 265-268.

10. Danell, A. S.; Parks J. H. Fraying and electron autodetachment dynamics of trapped gas phase oligonucleotides. *J. Am. Soc. Mass Spectrom.* **2003**, *14*, 1330-1339.

11. Anusiewicz, I.; Berdys-Kochanska J.; Czaplewski C.; Sobczyk M.; Daranowski E. M.; Skurski P.; Simons J. Charge loss in gas-phase multiply negatively charged oligonucleotides. *J. Phys. Chem. A* **2005**, *109*, 240-249.

12. Simons J. Anions. In *Encyclopedia of Mass Spectrometry Volume 1: Theory and Ion Chemistry*, Armentrout P. B., Ed.; Elsevier, 2003; pp. 55-68.

13. Yang, X.; Wang X. B.; Vorpagel E. R.; Wang L. S. Direct experimental observation of the low ionization potentials of guanine in free oligonucleotides by using photoelectron spectroscopy. *Proc. Natl. Acad. Sci. U. S A* **2004**, *101*, 17588-17592.

14. Rubio, M.; Roca-Sanjuan D.; Merchan M.; Serrano-Andres L. Determination of the lowest-energy oxidation site in nucleotides: 2 '-Deoxythymidine 5 '-monophosphate anion. *J. Phys. Chem. B* **2006**, *110*, 10234-10235.

15. Zakjevskii, V. V.; King S. J.; Dolgounitcheva O.; Zakrzewski V. G.; Ortiz J. V. Base and phosphate electron detachment energies of deoxyribonucleotide anions. *J. Am. Chem. Soc.* **2006**, *128*, 13350-13351.

16. Crecca, C. R.; Roitberg A. E. Theoretical Study of the Isomerization Mechanism of Azobenzene and Disubstituted Azobenzene Derivatives. *J. Phys. Chem. A* **2006**, *110*, 8188-8203.

17. Botan, V.; Backus E. H.; Pfister R.; Moretto A.; Crisma M.; Toniolo C.; Nguyen P. H.; Stock G.; Hamm P. Energy transport in peptide helices. *Proc. Natl. Acad. Sci. U. S A* **2007**, *104*, 12749-12754.

18. Lorquet, J. C. Whither the statistical theory of mass spectra. *Mass Spectrom. Rev.* **1994**, *13*, 233-257.

19. Boyall, D.; Reid K. L. Modern studies of intramolecular vibrational energy redistribution. *Chem. Soc. Rev.* **1997**, *26*, 223-232.

20. Nordholm, S.; Bäck A. On the role of nonergodicity and slow IVR in unimolecular reaction rate theory - A review and view. *Phys. Chem. Chem. Phys.* **2001**, *3*, 2289-2295.

21. Hu, Y. J.; Hadas B.; Davidovitz M.; Balta B.; Lifshitz C. Does IVR take place prior to peptide ion dissociation? *J. Phys. Chem. A* **2003**, *107*, 6507-6514.

22. Gruebele, M.; Wolynes P. G. Vibrational energy flow and chemical reactions. *Acc. Chem. Res.* **2004**, *37*, 261-267.

23. Schlag, E. W.; Selzle H. L.; Schanen P.; Weinkauf R.; Levine R. D. Dissociation Kinetics of Peptide Ions. *J. Phys. Chem. A* **2006**, *110*, 8497-8500.

24. Gregoire, G.; Kang H.; Dedonder-Lardeux C.; Jouvet C.; Desfrancois C.; Onidas D.; Lepere V.; Fayeton J. A. Statistical vs. non-statistical deactivation pathways in the UV photo-fragmentation of protonated tryptophan-leucine dipeptide. *Phys. Chem. Chem. Phys.* **2006**, *8*, 122-128.

25. Talbot, F. O.; Tabarin T.; Antoine R.; Broyer M.; Dugourd P. Photodissociation spectroscopy of trapped protonated tryptophan. *J. Chem. Phys.* **2005**, *122*, 074310.

26. Cosa, G.; Focsaneanu K. S.; Mclean J. R. N.; McNamee J. P.; Scaiano J. C. Photophysical properties of fluorescent DNA-dyes bound to single- and double-stranded DNA in aqueous buffered solution. *Photochem. Photobiol.* **2001**, *73*, 585-599.

27. Gorner, H. Direct and sensitized photoprocesses of bis-benzimidazole dyes and the effects of surfactants and DNA. *Photochem. Photobiol.* **2001**, *73*, 339-348.

28. Adhikary, A.; Buschmann V.; Müller C.; Sauer M. Ensemble and single-molecule fluorescence spectroscopic study of the binding modes of the bis-benzimidazole derivative hoechst 33258 with DNA. *Nucleic Acids Res.* **2003**, *31*, 2178-2186.

29. Ren, J.; Chaires J. B. Sequence and structural selectivity of nucleic acid binding ligands. *Biochemistry* **1999**, 16067-16075.

30. Wartell, R. M.; Larson J. E.; Wells R. D. Netropsin. A specific probe for A-T regions of duplex deoxyribonucleic acid. *J. Biol. Chem.* **1974**, *249*, 6719-6731.

31. Pilch, D. S.; Kirolos M. A.; Liu X.; Plum G. E.; Breslauer K. J. Berenil [1,3-Bis(4'-amidinophenyl)triazene] Binding to DNA Duplexes and to a RNA Duplex: Evidence for Both Intercalative and Minor Groove Binding Properties. *Biochemistry* **1995**, *34*, 9962-9976.

32. Doglia, S.; Graslund A.; Ehrenberg A. Binding of ethidium bromide to self-complementary deoxydinucleotides. *Eur. J. Biochem.* **1983**, *133*, 179-184.

33. Htun, T. A negative deviation from Stern-Volmer equation in fluorescence quenching. *J. Fluoresc.* **2004**, *14*, 217-222.

34. Sturgeon, R. J.; Schulman S. G. Electronic absorption spectra and protolytic equilibria of doxorubicin: direct spectrophotometric determination of microconstants. *J. Pharm. Sci.* **1977**, *66*, 958-961.

35. Chaires, J. B. Equilibrium studies on the interaction of daunomycin with deoxypolynucleotides. *Biochemistry* **1983**, *22*, 4204-4211.

36. *http://probes.invitrogen.com/handbook/;The Handbook - A Guide to Fluorescent Probes and Labeling Technologies* Invitrogen: 2006.

37. Marras, S. A. E.; Kramer F. R.; Tyagi S. Efficiencies of fluorescence resonance energy transfer and contact-mediated quenching in oligonucleotide probes. *Nucleic Acids Res.* **2002**, *30*, e122.

38. Velapoldi, R. A.; Tonnesen H. H. Corrected emission spectra and quantum yields for a series of fluorescent compounds in the visible spectral region. *J. Fluoresc.* **2004**, *14*, 465-472.

39. Magde, D.; Wong R.; Seybold P. G. Fluorescence quantum yields and their relation to lifetimes of rhodamine 6G and fluorescein in nine solvents: Improved absolute standards for quantum yields. *Photochem. Photobiol.* **2002**, *75*, 327-334.

40. Trotta, E.; D'Ambrosio E.; Ravagnan G.; Paci M. Evidence for DAPI intercalation in CG sites of DNA oligomer $[d(CGACGTCG)]_2$: a ^1H NMR study. *Nucleic Acids Res.* **1995**, *23*, 1333-1340.

41. Colson, P.; Houssier C.; Bailly C. Use of Electric Linear Dichroism and competition Experiments with Intercalating Drugs to Investigate the Mode of Binding of Hoechst 33258, Berenil and DAPI to GC Sequences. *J. Biomol. Struc. Dyn.* **1995**, *13*, 351-365.

42. Rosu, F.; Pirotte S.; De Pauw E.; Gabelica V. Positive and negative ion mode ESI-MS and MS/MS for studying drug–DNA complexes. *Int. J. Mass Spectrom.* **2006**, *253*, 156-171.

43. Okumura, Y.; Yeh L. I.; Myers J. D.; Lee Y. T. Infrared spectra of the cluster ions $H_7O_3^+.H_2$ and $H_9O_4^+.H_2$. *J. Chem. Phys.* **1986**, *85*, 2328-2329.

44. Oomens, J.; Polfer N.; Moore D. T.; van der Meer L.; Marshall A. G.; Eyler J. R.; Meijer G.; von Helden G. Charge-state resolved mid-infrared spectroscopy of a gas-phase protein. *Phys. Chem. Chem. Phys.* **2005**, *7*, 1345-1348.

45. Danell, A. S.; Parks J. H. FRET measurements of trapped oligonucleotide duplexes. *Int. J. Mass Spectrom.* **2003**, *229*, 35-45.

46. Norman, D. G.; Grainger R. J.; Uhrin D.; Lilley D. M. J. Location of cyanine-3 on double-stranded DNA: Importance for fluorescence resonance energy transfer studies. *Biochemistry* **2000**, *39*, 6317-6324.

47. Reha, D.; Kabelac M.; Sponer J.; Sponer J. E.; Elsner M.; Suhai S.; Hobza P. Intercalators. 1. Nature of stacking interactions between intercalators (Ethidium, Daunomycin, Ellipticine, and 4',6-Diaminide-2-phenylindole) and DNA Base pairs. Ab initio quantum chemical, density functional theory, and empirical potential study. *J. Am. Chem. Soc.* **2002**, *124*, 3366-3376.

48. O'Neill M. A.; Barton J. K. Sequence-dependent DNA dynamics: the regulator of DNA-mediated charge transport. In *Charge transfer in DNA: from mechanisms to application*, Wagenknecht H. A., Ed.; Wiley-VCH: Weinheim, 2005; pp. 27-75.

49. Kelley, S. O.; Holmlin R. E.; Stemp E. D. A.; Barton J. K. Photoinduced electron transfer in ethidium-modified DNA duplexes: Dependence on distance and base stacking. *J. Am. Chem. Soc.* **1997**, *119*, 9861-9870.

50. Kelley, S. O.; Barton J. K. DNA-mediated electron transfer from a modified base to ethidium: pi-stacking as a modulator of reactivity. *Chem. Biol.* **1998**, *5*, 413-425.

51. Bossio, R. E.; Hudgins R. R.; Marshall A. G. Gas phase photochemistry can distinguish different conformations of unhydrated photoaffinity-labeled peptide ions. *J. Phys. Chem. B* **2003**, *107*, 3284-3289.

52. Förster, T. Energiewanderung und Fluoreszenz. *Naturwissenschaften* **1946**, *6*, 166-175.

53. Clegg, R. M. Fluorescence resonance energy transfer and nucleic acids. *Methods Enzymol.* **1992**, *211*, 353-388.

54. Khoury, J. T.; Rodriguez-Cruz S. E.; Parks J. H. Pulsed fluorescence measurements of trapped molecular ions with zero background detection. *J. Am. Soc. Mass Spectrom.* **2002**, *13*, 696-708.

55. Friedrich, J.; Fu J. M.; Hendrickson C. L.; Marshall A. G.; Wang Y. S. Time resolved laser-induced fluorescence of electrosprayed ions confined in a linear quadrupole trap. *Rev. Sci. Instrum.* **2004**, *75*, 4511-4515.

56. Frankevich, V.; Guan X. W.; Dashtiev M.; Zenobi R. Laser-induced fluoresence of trapped gas-phase molecular ions generated by internal-source matrix-assisted laser desorption/ionization in a Fourier transform ion cyclotron resonance mass spectrometer. *Eur. J. Mass Spectrom.* **2005**, *11*, 475-482.

57. Iavarone, A. T.; Duft D.; Parks J. H. Shedding light on biomolecule conformational dynamics using fluorescence measurements of trapped ions. *J. Phys. Chem. A* **2006**, *110*, 12714-12727.

58. Dashtiev, M.; Azov V.; Frankevich V.; Scharfenberg L.; Zenobi R. Clear evidence of fluorescence resonance energy transfer in gas-phase ions. *J. Am. Soc. Mass Spectrom.* **2005**, *16*, 1481-1487.

59. Antony, T.; Subramanian V. Molecular beacons: nucleic acid hybridization and emerging applications. *J. Biomol. Struct. Dyn.* **2001**, *19*, 497-504.

60. Fang, X.; Li J. J.; Perlette J.; Tan W.; Wang K. Molecular beacons. Novel fluorescent probes. *Anal. Chem.* **2000**, 747 A-753 A.